WAVE FORCES EXERTED ON SUBMERGED CIRCULAR CYLINDERS FIXED IN DEEP WAVES

Koterayama, Wataru
Research Institute for Applied Mechanics, Kyushu University : Associate Professor

https://doi.org/10.5109/6617924

出版情報：Reports of Research Institute for Applied Mechanics. 27 (84), pp.25-46, 1979-09. 九州大学応用力学研究所
バージョン：
権利関係：

Reports of Research Institute for Applied Mechanics
Vol. XXVII, No. 84, 1979

WAVE FORCES EXERTED ON SUBMERGED CIRCULAR CYLINDERS FIXED IN DEEP WAVES*

Wataru KOTERAYAMA**

Wave forces exerted on circular cylinders in deep waves are investigated. The circular cylinders are fixed horizontally below the water surface.

Experimental results are compared with values calculated by linear theory and the other data obtained differently.

Main conclusions obtained are as follows:

1) In case of small period paramaters, inertia coefficients obtained by experiments show good agreement with theoretical values calculated by linear theory. But for large period parameters, the experimental values are much smaller than the theoretical ones.

2) For large period parameters, Drag coefficients derived in the present investigation approximately coincide with those obtained in experiments on hydrodynamic forces acting on circular cylinders in oscillatory flow. But there is much difference between them in case of not so large period parameters.

Key words: Drag and inertia coefficients, Horizontal cylinders, Deep wave

1. Introduction

Many theoretical and experimental studies show that wave forces acting on a ship can be estimated accurately by linear theory. But linear theory can not be used for calculating wave forces exerted on a body of which the dimension is small as compared with incident wave heights. An occean structure is usualy composed of many pipes, and their diameters are not so large as ship's breadth, so we should calculate wave loads by the other method.

The investigations on methods of estimating wave loads acting on an ocean structure were carried out by Morison[1] and the other many researchers[2)-8)]. But their interests were mainly on a vertical cylinder fixed in shallow sea, so they measured the force acting on a circular cylinder in the flow field which simulate those of the shallow sea. For example, Keulegan

* This paper is translated from J. S. N. A. of Japan, Vol. 143 (1978)

** Associate Professor, Research Institute for Applied Mechanics, Kyushu University.

and Carpenter[2] measured forces acting on horizontal cylinders fixed in simple sinusoidal currents in standing waves. The experiment showed that the drag and the inertia coefficients depend on a period parameter $Kc=UmT/D$ (Um: semiamplitude of the current, T: the period of the alternation, D: the diameter of the cylinder). T. Sarpkaya[3),4)] investigated on circular cylinders fixed in a harmonically oscillating fluid in a large U-shaped vertical tunnel, and he obtained same results as those of Keulegan-Carpenter. Nowadays, ocean structures are constructed in relatively deep sea and they are composed of not only vertical cylinders but aslo horizontal ones.

In a deep wave, the fluid particle makes a orbital motion, therefore the flow direction to the horizontal cylinder is always changed. As a drag force is in proportion to the square of the velocity, the vertical component of the flow velocity has relation to the horizontal drag force. On the other hand, the drag force acting on a vertical cylinder even in the deep wave is approximately related to only the horizontal component of a orbital velocity. There are few studies on the limit of applicability of linear theory and its correction method which should be very useful for a designer of ocean structures.

In this paper, wave forces exerted on submerged horizontal circular cylinders in deep waves are investigated, and the experimental results are compared with values calculated by linear theory and the other data obtained by Keulegan-Carpenter[2] and Sarpkaya[3].

2. Experimental arrangement

Experiments are carried out at the towing tank, $L\times B\times D=80\text{m}\times 8\text{m}\times 3$ m of Research Institute for Applied Mechanics of Kyushu University. The

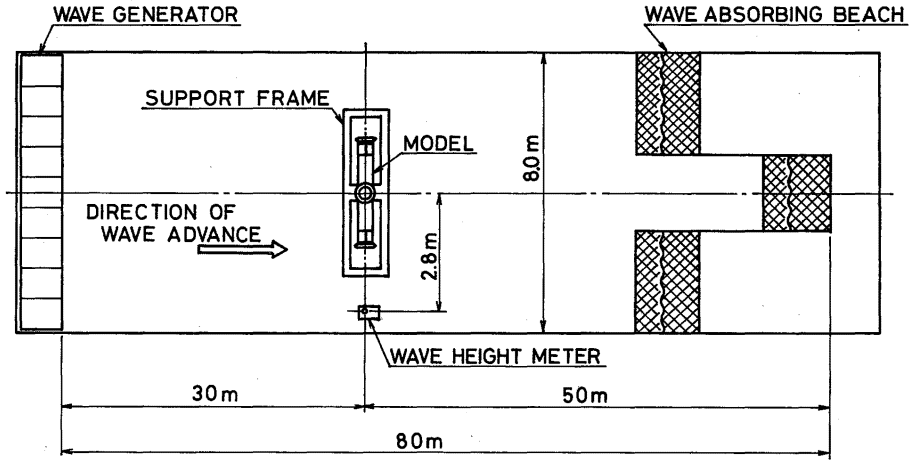

Fig. 1 Experimental setup

immersed depths of models are 0.2m. Experimental views are shown in Fig. 1 and Photo. 1. Incident wave heights are measured by a servo-type wave height meter. Table 1 contains the diameters of circular cylinders, the wave periods and the wave heights. A fluid particle velocity and acceleration can be calculated by linear wave theory with enough accuracy in the range of these wave periods and heights.

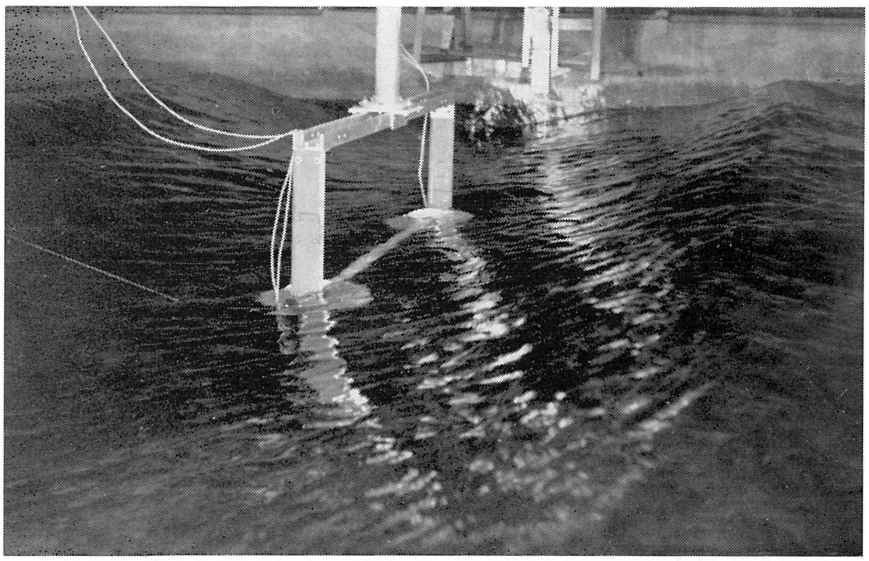

Photo. 1 A view of experimental run

The studies on the vertical cylinders found that wave forces are strongly correlated with the period parameter. Then the period parameters of models are necessarily equal to those of a ocean structure. So the diameters of models are decided according to the ability of our wave maker. They are selected as shown in Table 1.

The end effect of a circular cylinder on the drag force can not be ignored[9]. Then the end plates shown in Fig. 2 are fixed to the models to prevent the three dimensional effect. The sketch of the dynamometer assembly is shown in Fig. 2. The inertia and the drag coefficients are obtained from measured forces by subtracting the forces acting on the end plates and the dynamometers, which were measured separately. The dynamometers were calibrated by loading the models. Natural frequencies of the dynamometers fixed to the models are enough high as compared with the wave periods.

Table 1 Wave period T and wave height H_w

	T(sec)	1.00	1.06	1.20	1.24	1.35	1.45	1.55	1.60	1.80	1.95	2.10	2.20	2.40
Model 1		0.038	0.040	0.042	0.040	0.042	0.040	0.038	0.038	0.034	0.030	0.028		0.024
$D=0.08$ m	H_w(m)	0.094		0.142	0.152	0.172	0.190	0.210	0.212	0.212	0.204	0.194		0.160
					0.202		0.260			0.312		0.272		0.224
Model 2				0.046	0.044	0.040	0.040	0.036	0.036	0.032	0.030	0.028		0.022
$D=0.019$ m	H_w(m)	0.084		0.134	0.146	0.168	0.188	0.210	0.210	0.216	0.204	0.186	0.180	0.152
				0.184	0.196	0.236								0.220
Model 3		0.040	0.040	0.044	0.042	0.040	0.040	0.038	0.036	0.032	0.030			
$D=0.010$ m	H_w(m)			0.134	0.144	0.166	0.186	0.208	0.210	0.224	0.208	0.192	0.178	0.156
				0.192	0.198	0.230	0.246	0.260	0.272	0.294	0.288	0.266	0.250	

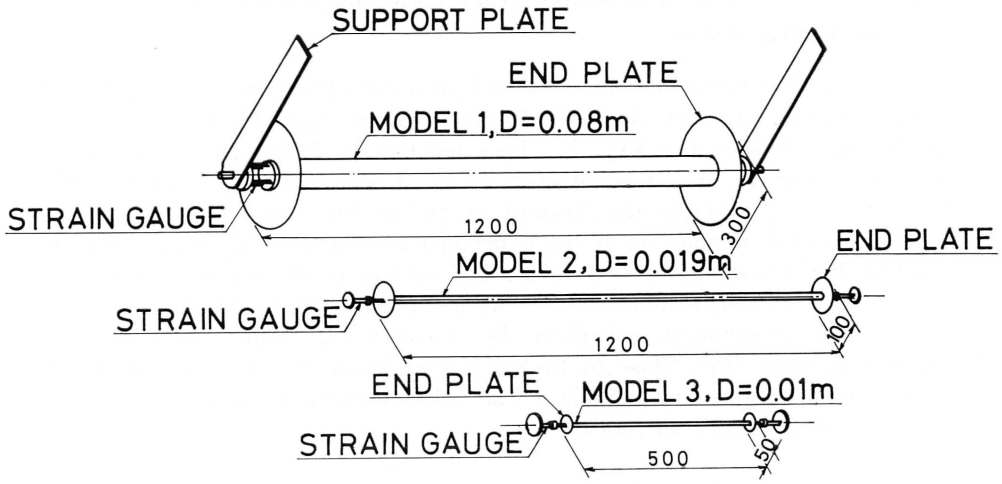

Fig. 2 Model and dynamometer

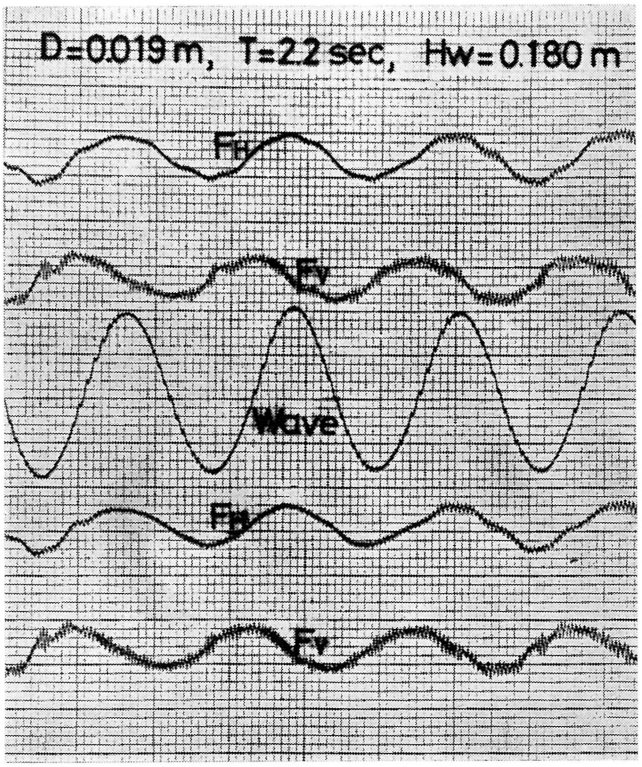

Fig. 3 Records of wave forces and wave profile

3. Analysis of the experimental results and comparison with the theoretical results

Results of experiments are recorded on a data recorder and analized by using a digital computer (FACOM 230-48). Some examples of records on a oscillogram are shown in Fig. 3. Two records of forces in the figure are those measured by two dynamometers fixed to both ends of a model. The forces acting on a model are obtained by adding two measured forces.

The method of analysis of the experimental results is shown as follows. Take O_y horizontal and in the undisturbed surface of the water, and O_z vertical upward as shown in Fig. 4. As mentioned before, the fluid particle velocity and acceralation calculated by linear wave theory deviate only 3 parcents at most from those by Stokes wave theory in the range of experimented wave heights and periods. The velocity potential of a wave is given by linear wave theory as follows.

$$\phi=-\frac{g\zeta_a}{\omega}\cdot e^{Kz}\cdot\cos(Ky-\omega t), \tag{1}$$

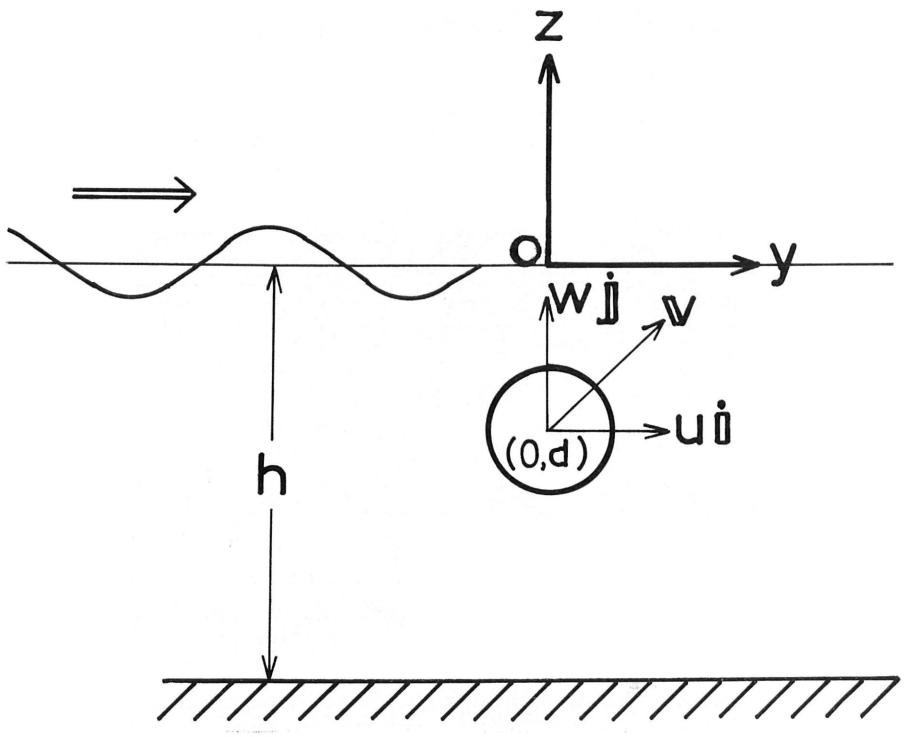

Fig. 4 Coordinate system

where ω is the circular frequency, K equals to ω^2/g and ζ_a is the semiamplitude of a wave. A wave profile is written as

$$\zeta=-\frac{1}{g}\left(\frac{\partial\phi}{\partial t}\right)_{z=0}=\zeta_a\sin(Ky-\omega t). \tag{2}$$

Fluid particle velocities and acceralations are written as

$$\left.\begin{aligned} u&=\frac{\partial\phi}{\partial y}=\omega\zeta_a\cdot e^{Kz}\cdot\sin(Ky-\omega t)\\ w&=\frac{\partial\phi}{\partial z}=-\omega\zeta_a\cdot e^{Kz}\cdot\cos(Ky-\omega t)\\ \dot{u}&=\frac{\partial u}{\partial t}=-\omega^2\zeta_a\cdot e^{Kz}\cdot\cos(Ky-\omega t)\\ \dot{w}&=\frac{\partial u}{\partial t}=-\omega^2\zeta_a\cdot e^{Kz}\cdot\sin(Ky-\omega t) \end{aligned}\right\}. \tag{3}$$

A velocity vector at the center of the circular cylinder is denoted as follows.

$$\boldsymbol{V}=(u\boldsymbol{i}+w\boldsymbol{j})_{y=0,z=\bar{d}} \tag{4}$$

The wave force acting on a submerged horizontal circular cylinder is given by linear theory[10] as follows.

$$\begin{aligned} \boldsymbol{F}&=F_H\boldsymbol{i}+F_V\boldsymbol{j}\\ &=L\left(a_y\frac{\pi D^2}{4}\dot{u}+\oint P_y ds+b_y u\right)\boldsymbol{i}\\ &+L\left(a_z\frac{\pi D^2}{4}\dot{w}+\oint P_z ds+b_z w\right)\boldsymbol{j} \end{aligned} \tag{5}$$

where the first and third terms in two parentheses denote the diffraction forces and the second is Froude-Kriloff's force. The first term has the same phase as the second term has. So it can be rewritten as follows.

$$\begin{aligned} F&=L\left(\rho C_{MH}\frac{\pi D^2}{4}\dot{u}+b_y u\right)\boldsymbol{i}\\ &+L\left(\rho C_{MV}\frac{\pi D^2}{4}\dot{w}+b_z w\right)\boldsymbol{j}, \end{aligned} \tag{6}$$

where C_{MH} and C_{MV} are inertia coefficients along the axes y and z. In viscouse flow, the term which is in proportion to the square of the flow velocity should be added to eq. (6).

$$F=L\left(\rho C_{MH}\frac{\pi D^2}{4}\dot{u}+b_y u\right)\boldsymbol{i}$$
$$+L\left(\rho C_{MV}\frac{\pi D^2}{4}\dot{w}+b_z w\right)\boldsymbol{j}$$
$$+\frac{1}{2}\rho C_D DL|\boldsymbol{V}|\boldsymbol{V}$$
$$=L\left(\rho C_{MH}\frac{\pi D^2}{4}\dot{u}+b_y u+\frac{1}{2}\rho C_D D\sqrt{u^2+w^2}u\right)\boldsymbol{i}$$
$$+L\left(\rho C_{MV}\frac{\pi D^2}{4}\dot{w}+b_z w+\frac{1}{2}\rho C_D D\sqrt{u^2+w^2}w\right)\boldsymbol{j}, \tag{7}$$

where C_D is the drag coefficient. Morison's equation is used for calculating the wave force acting on a vertical cylinder and it ignores the second term in the parentheses in eq. (7). Then the first order horizontal and vertical wave force are obtained by substituting eq. (3) and $y=0$, $z=d$ into eq. (7) as follows.

$$F_{H1}=\rho C_{MH}\frac{\pi D^2}{4}L(-\omega^2\zeta_a e^{Kd}\cos\omega t)$$
$$-\omega\zeta_a e^{Kd}b_y L\sin\omega t$$
$$-\frac{1}{2}\rho C_D DL\omega^2\zeta_a^2 e^{2Kd}\sin\omega t \tag{8}$$

$$F_{V1}=\rho C_{MV}\frac{\pi D^2}{4}L(\omega^2\zeta_a e^{Kd}\sin\omega t)$$
$$-\omega\zeta_a e^{Kd}b_z L\cos\omega t$$
$$-\frac{1}{2}\rho C_D DL\omega^2\zeta_a^2 e^{2Kd}\cos\omega t \tag{9}$$

Mesured forces usually contain higher order terms, so they may be expanded into Fourier series as

$$\left.\begin{aligned}F_H&=\sum_{n=0}^{R}F_{Hn}=\sum_{n=0}^{R}(A_{Hn}\sin n\omega t+B_{Hn}\cos n\omega t)\\F_V&=\sum_{n=0}^{R}F_{Vn}=\sum_{n=0}^{R}(A_{Vn}\sin n\omega t+B_{Vn}\cos n\omega t)\end{aligned}\right\} \tag{10}$$

Next the values of $\bar{F}_{H1}$, C_{MH} and C_{DH} can be obtained from A_{H1} and B_{H1} on the basis of eq. (8), the values of $\bar{F}_{V1}$, C_{MV} and C_{DV} can be obtained from A_{V1} and B_{V1} on the basis of eq. (9), where $\bar{F}_{H1}$ and $\bar{F}_{V1}$ are nondimensional first order wave forces and C_{DH}, C_{DV} are drag coefficients obtained from horizontal and vertical forces respectively.

It can be found out from eq. (8) and (9) that the velocity components of the diffraction force can not be distinguished experimentally from the drag forces. In this paper, the drag forces are obtained from the measured forces by subtracting the velocity components of the diffraction forces calculated by linear theory. Experiments show that the diffraction force can not be calculated acculately by linear theory in case of large period parameters. But, in such case, the velocity component of diffraction forces are very small as compared with the drag force. So the method of data analysis proposed here is useful not only in case of small period parameter but also in case of large one. In these experiments, the velocity components of the diffraction forces are not more than 10 percents of the drag forces in case of model 1, and 1 percent in case of model 2 and model 3. If they were ignored in case of small period parameter, the drag coefficients can not be obtained accurately. The calculated values by linear theory are obtained by using the close fit method[11] in which singularities are distributed on the surface of a circular cylinder.

The following relations are found out by linear theory for the submerged circular clylinder.

$$C_{MH}=C_{MV},\ b_y=b_z \tag{11}$$

Finally the coefficients are obtained as follows.

$$\left.\begin{aligned}
\bar{F}_{H_1}&=\frac{|\boldsymbol{F}_{H_1}|}{\rho g\zeta_a DL}=\frac{\sqrt{A^2{}_{H_1}+B^2{}_{H_1}}}{\rho g\zeta_a DL}\\
C_{MH}&=\frac{B_{H_1}\cos\omega t}{\rho\frac{\pi D^2}{4}L\dot{u}}=\frac{-B_{H_1}}{\rho\frac{\pi D^2}{4}L\omega^2\zeta_a e^{Kd}}\\
C_{DH}&=\frac{A_{H_1}\sin\omega t-b_y uL}{\frac{1}{2}\rho DL|\boldsymbol{V}|u}=\frac{-A_{H_1}-b_y L\omega\zeta_a e^{Kd}}{\frac{1}{2}\rho DL\omega^2\zeta_a^2 e^{2Kd}}\\
\bar{F}_{V_1}&=\frac{|\boldsymbol{F}_{V_1}|}{\rho g\zeta_a DL}=\frac{\sqrt{A^2_{V_1}+B^2_{V_1}}}{\rho g\zeta_a DL}\\
C_{MV}&=\frac{A_{V_1}\sin\omega t}{\rho\frac{\pi D^2}{4}L\dot{w}}=\frac{A_{V_1}}{\rho\frac{\pi D^2}{4}L\omega^2\zeta_a e^{Kd}}\\
C_{DV}&=\frac{B_{V_1}\mathrm{con}\,\omega t-b_z uL}{\frac{1}{2}\rho DL|\boldsymbol{V}|w}=\frac{-B_{V_1}-b_z\omega\zeta_a e^{Kd}}{\frac{1}{2}\rho DL\omega^2\zeta_a^2 e^{2Kd}}
\end{aligned}\right\} \tag{12}$$

Measured wave forces and the composit values by eq. (10) are shown in Fig. (5). In case the wave height is small (Fig. 5. (a)), the phase difference between the wave profile and the horizontal component of the wave force is 90°, then it is found out that the inertia force is dominant. In case

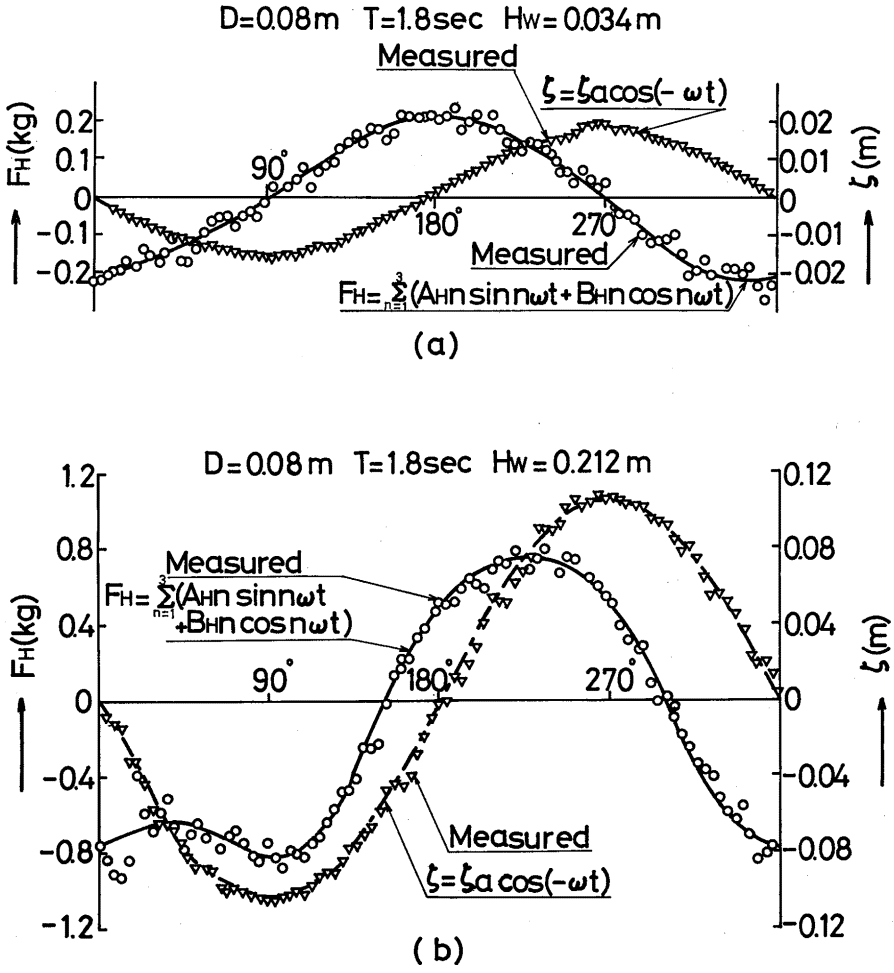

Fig. 5 Comparison between measured values and calculated ones by *eq.* (10)

of the large wave height (Fig. 5. (b)), the phase difference is 30°, and the experiment indicates that the drag force is greater than the inertia force. In latter case, the wave force contains the second and third order term as shown in Fig. 5(b).

Figures 6 and 7 show C_{MH} and C_{MV} of the model 1, 2, 3 as a function $\xi_D=\frac{KD}{2}$. As the wave lengths are much greater than the diameters of models in these experiments, the calculated results by linear theory is nearly equal to 2.0. The calculated results are agree with those of experiments in case of small period parameter. But the calculated results are much greater

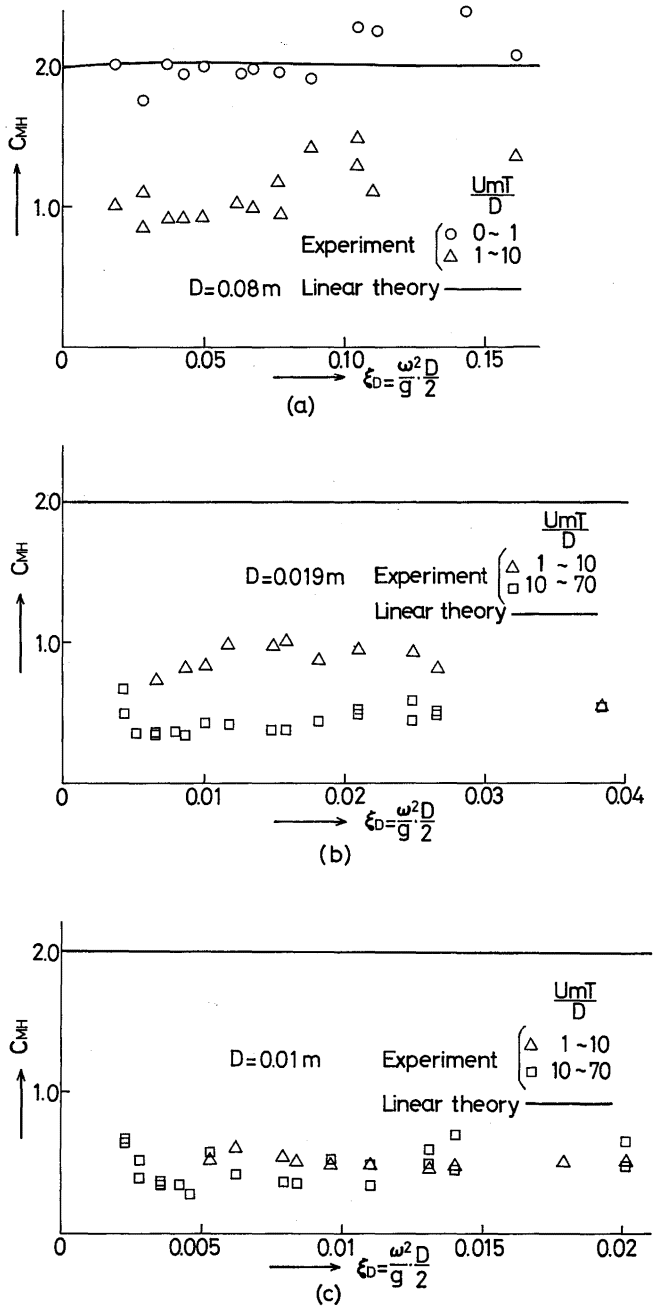

Fig. 6 Inertia component of horizontal wave force, C_{MH}

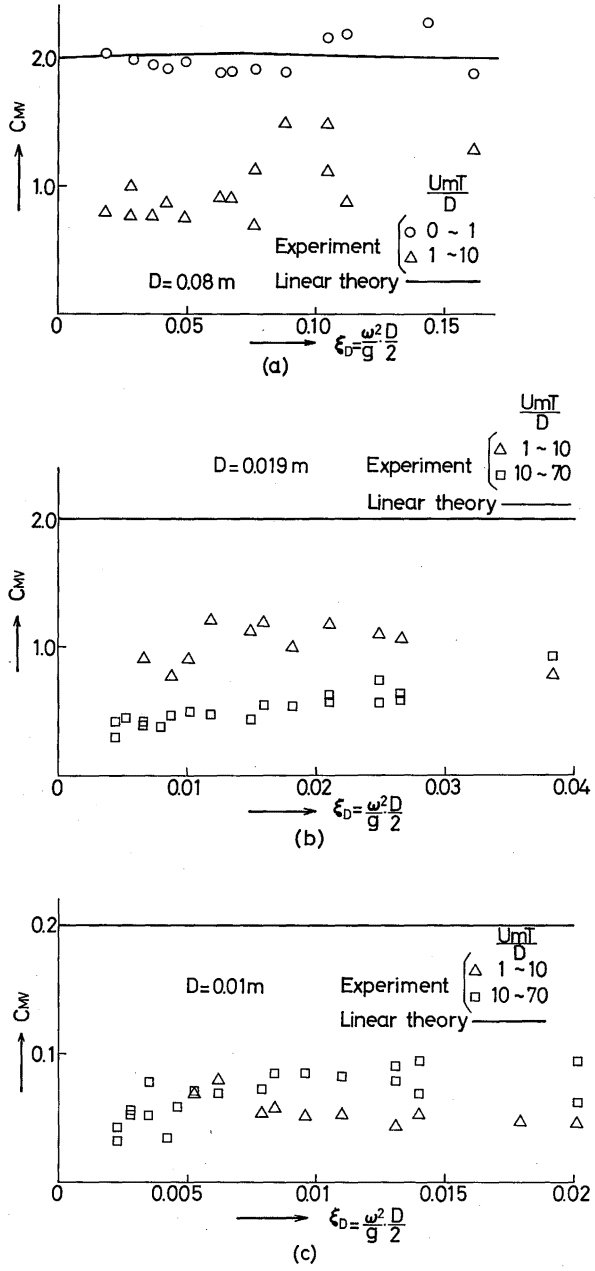

Fig. 7 Inertia component of vertical wave force, C_{MV}

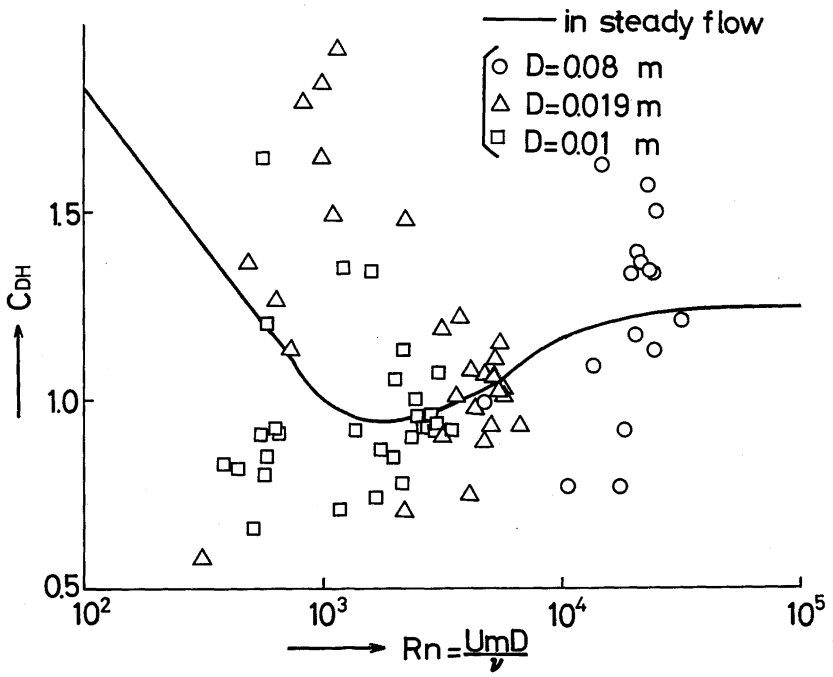

Fig. 8 Drag component of horizontal wave force, C_{DH}

than those of experiments in case of large period parameter. Through the all range of period parameter, the experiments show that C_{MH} equals to C_{MV} as indicated by linear theory.

Figures 8 and 9 show the experimental results of C_{DH} and C_{DV} as a function of $R_n=\frac{U_mD}{\nu}$ together with the drag coefficient in steady flow[12]. The experiments show that the drag coefficients in waves are not only function of Reynolds number.

As shown in eq. (7), the distinction between C_{DH} and C_{DV} is not in their natures but in their methods of the calculation. Moreover, the results of experiments show that there is not large difference between their values. So the mean of their values may be written as C_D of these models. As for the inertia coefficients C_{MH} and C_{MV}, the same fact can be derived from linear theory and experiments. Figures 10 and 11 show C_M and C_D as a function of period parameter K_C. In these figures, dotted lines show the experimental result by Keulegan-Carpenter[2] in simple sinusoidal currents in standing waves and chain lines show the value obtained by Sarpkaya[3] in harmonically oscillating fluid in a U-shaped vertical tunnel. Solid lines show the mean value of present experiments in deep waves. The wave forces acting on model 2 and 3 are very small in case of $K_C<10$, so in this region,

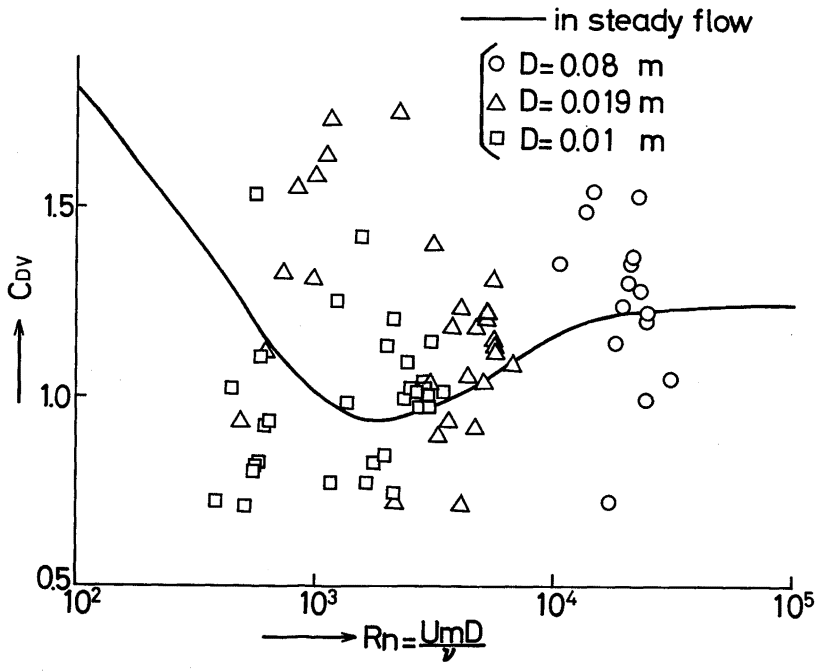

Fig. 9 Drag component of vertical wave force, C_{DV}

the solid line is drawn as a mean line of the results of model 1.

It is well-known that the drag force of a blunt body is due to flow separation and resulting vortex formation. The relation between the vortex formation and period parameter K_C is studied here on the basis of the Navier-Stokes equation.

The two dimensional form of the Navier-Stokes equation describing the flow of an incompressible fluid is,

$$\frac{\partial \eta}{\partial t}+\frac{\partial (u\eta)}{\partial y}+\frac{\partial (w\eta)}{\partial z}=\nu \Delta^2 \eta, \tag{13}$$

where η is the vorticity and t is time. The following nondimensionalization is introduced.

$$\bar{y}=\frac{y}{D},\ \bar{z}=\frac{z}{D},\ \bar{u}=\frac{u}{U_m},\ \bar{w}=\frac{w}{U_m},\ \bar{t}=\frac{t}{T},\ \bar{\eta}=\frac{D}{U_m}\eta,$$

where U_m equals to $\omega \zeta_a e^{Kd}$ and T is wave period. In terms of these dimensionless variables, equation (13) yields the following equation.

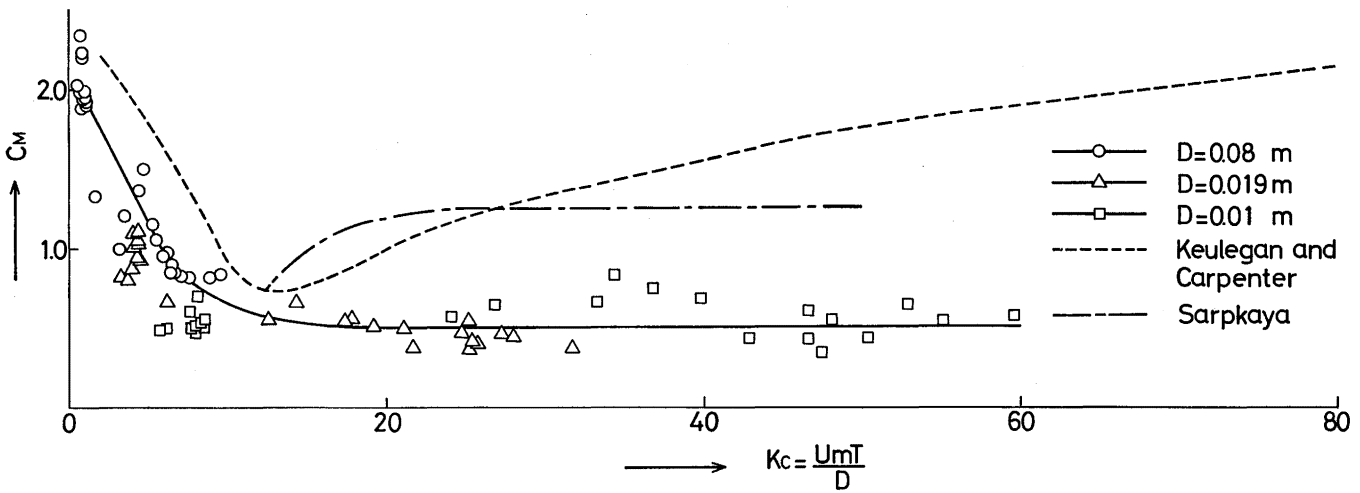

Fig. 10 Inertia coefficient, C_M

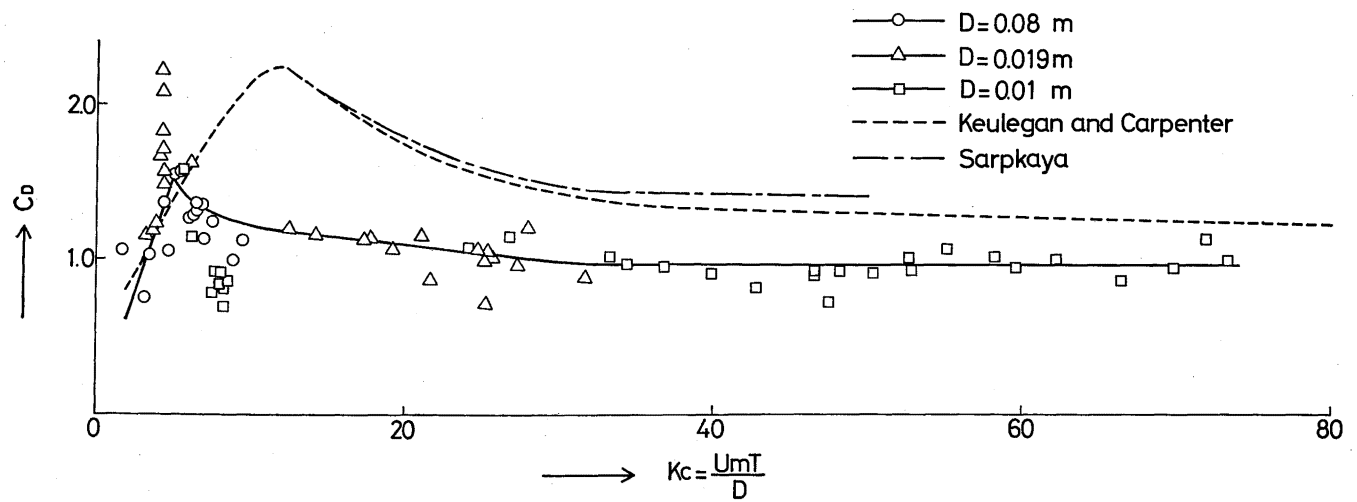

Fig. 11 Drag coefficient, C_D

$$\frac{\partial \bar{\eta}}{\partial \bar{t}}+K_c\cdot\frac{\partial(\bar{u}\bar{\eta})}{\partial \bar{y}}+K_c\cdot\frac{\partial(\bar{w}\bar{\eta})}{\partial \bar{z}}=\frac{1}{R_n}\cdot K_c\Delta^2\bar{\eta} \tag{14}$$

Equation (14) shows that the flow field can be characterized by nondimensional parameters R_n and K_c. The correlation of the flow field with period parameter K_c is studied in case of large R_n number ($R_n\gg 1$).

In case of $K_c\ll 1$

$$\frac{\partial \bar{\eta}}{\partial \bar{t}}=0 \tag{15}$$

In this region, the vortex shedding is not found out and the flow field is the same as that in nonviscouse flow except very near the wall. Therefore the calculated results of inertia coefficients by linear theory agree with the experimental ones in case of small K_c. The experiment by M. Schwabe[13] showed that the drag coefficient C_D is very small in case of small period parameter. As for a model which has corners or sharp edges, the second or third term and the right hand side of eq. (14) become locally great large. So eq. (15) does not hold good in such a case. Present paper does not deal with the case.

In case of $K_c\sim 1$ ($1<K_c<30$ is experimentally found)

$$\frac{\partial \bar{\eta}}{\partial \bar{t}}+K_c\cdot\frac{\partial(\bar{u}\bar{\eta})}{\partial \bar{y}}+K_c\cdot\frac{\partial(\bar{w}\bar{\eta})}{\partial \bar{z}}=0 \tag{16}$$

The period parameter K_c has large effect on the flow field. Evidently, the vorticity $\bar{\eta}$ is generated by the action of viscosity, so the Reynolds effect should not be ignored.

Honji and Taneda[14] investigated experimentally the symmetrical unsteady vortices behind a circular cylinder started from rest either impulsively or with uniform acceleration using a flow visualization technique, and the following conclusions for the length S of the vortices were obtained.

In case of $K_n<1$ $S=0$ (where $K_n\fallingdotseq K_c/\pi$)

In case of $1<K_n<10$ $S\propto K_n$

This relation hold in a limit of R_n number. The maximum period parameter K_{nmax} beyound which the stable symmetrical two vortices are not formed hehind a cylinder decreases with increasing R_n number. For example, K_{nmax} equals to 10 in case R_n number is 10^2, and K_{nmax} equals to 4 in case R_n number is 10^3.

It is well-known fact that the stable symmetrical two vortices can not formed behind a circular cylinder in steady flow at $R_n>40$, so it may be said that the vortices in unsteady flow are stabler than those in steady flow. The drag coefficiet C_D in steady flow at $R_n=40$ is nearly equal to 2.0 and it is very interesting that the value agrees with those maximum values

obtained by Keulegan-Carpenter's and Sarpkaya's experiments. The fluid particle in both experiments makes simple harmonic motions on a straight line, which is different from those of Honji's experiment. But we may deduce from Honji's experiment that the large value ($C_D=2.0$) is due to the stable vortices which do not exsist in steady flow at $R_n>40$. In present experiments in deep waves, the absolute velocity at a point is independent of time and only its direction is variable with time. The formed vortices do not depart from but move round a circular cylinder in this range of period parameter. In this range of period parameter, the flow fields in deep waves are quite different from those of simple harmonic motions on a straight line, where the formation, diffusion and dissipation of vortices are periodicaly observed. Therefore the results of present experiments for the drag coefficient naturally do not agree with those of the other experiments in case of $1<K_c<30$.

In case of $K_c\gg 1$ ($K_c>30$ is experimentally found)

$$\frac{\partial(\bar{u}\bar{\eta})}{\partial\bar{y}}+\frac{\partial(\bar{w}\bar{\eta})}{\partial\bar{z}}=\frac{1}{R_n}\Delta^2\bar{\eta} \tag{17}$$

The flow field depends mainly on R_n number in this region. In this case, the regular Karman vortices are separated from the cylinder in deep wave, oscillating fluid and standing wave. The vortex distribution near the cylinder at enough large K_c in each flow field should resemble that in steady flow because the period of each flow field is much longer than that of Karman vortex. The difference between C_D or C_M obtained by present study and those by the other experiments is seemingly due to Reynolds effect. The drag coefficient C_D obtained by Keulegan-Carpenter at $K_c>30$ is 1.3 and that by Sarpkaya is 1.4. The model section used by Sarpkaya is too large for his water tunnel and the wall-effect can not be ignored. The drag coefficient becomes 1.26 after correcting. The Reynolds numbers at $K_c>30$ in their experiment are around 10^4 and the drag coefficient at the same Reynolds number in steady flow is 1.25. The drag coefficient obtained by present experiment at $K_c>30$ is 1.0 and the Reynolds number is around 5×10^3. The drag coefficient at the same R_n number in steady flow is 1.05. Then the drag coefficient in each experiment at large K_c approximately agrees with that in steady flow.

As for the inertia coefficient C_M, there are large differencies among three experiments. Sarpkaya showed that C_M decreases with decreasing R_n number. The difference between C_M by Sarpkaya and that by author may be partly explained by above reason. The present experiment shows that C_M at $K_c>20$ does not vary with K_c.

The ratio of the inertia force to the drag force can be obtained from eq. (8) as follows.

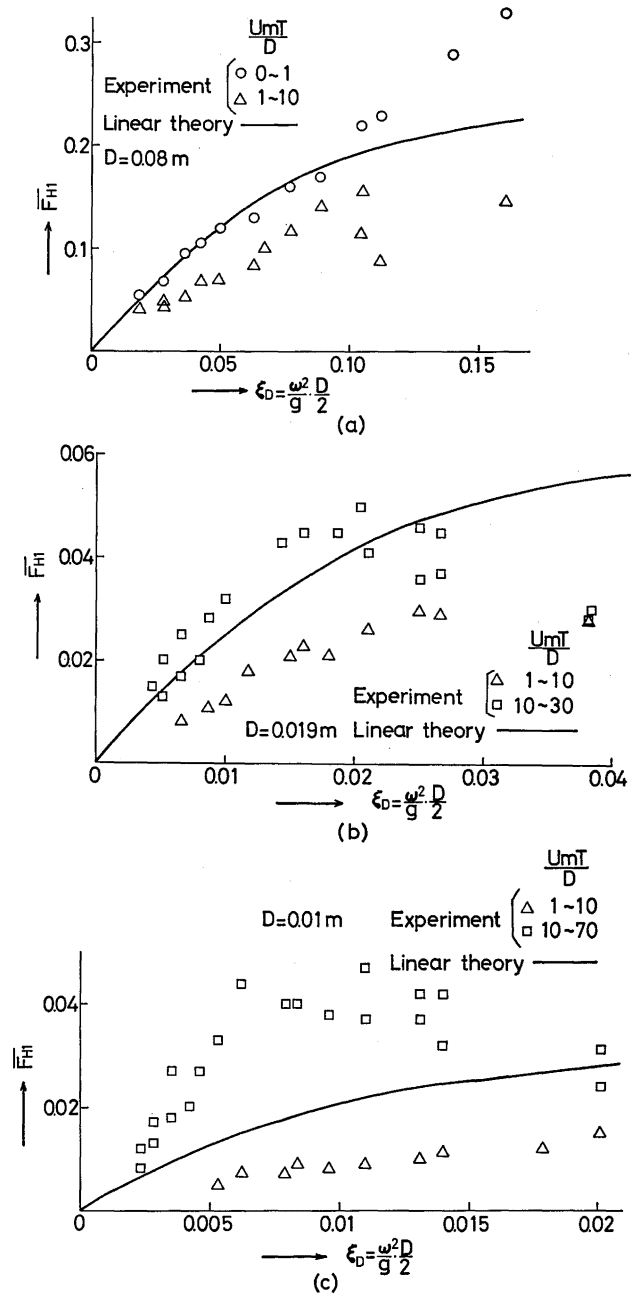

Fig. 12 First order wave force coefficient, $\bar{F}_{H1}$

$$\frac{|F_M|}{|F_D|} \doteqdot \frac{\pi^2}{K_c} \cdot \frac{C_M}{C_D} \tag{18}$$

In case of very small K_c, drag force F_D is much smaller than inertia force F_M and the drag coefficient C_D can not be obtained accurately. In case of large K_c, inertia force F_M is much smaller than F_D. Therefore, the drag coefficient C_D at $K_c<2$ and the inertia coefficient C_M at $K_c>60$ are not shown in Fig. 11 and Fig. 10.

Figure 12 shows the nondimensional horizontal wave force $\overline{F_{H1}}$ as a function of ξ_D. The solid lines in the figure indicate the calculated results by linear theory. The calculated results by linear theory agree with those of experiments at $K_c<1$. The calculated results are greater than experimental ones at $1<K_c<10$ because calculated inertia forces are greater than experimental ones. In case $K_c>10$, the calculated results are smaller than experimental ones because the drag forces become dominant.

Figure 13 shows second terms of wave forces nondimensionalized as follows.

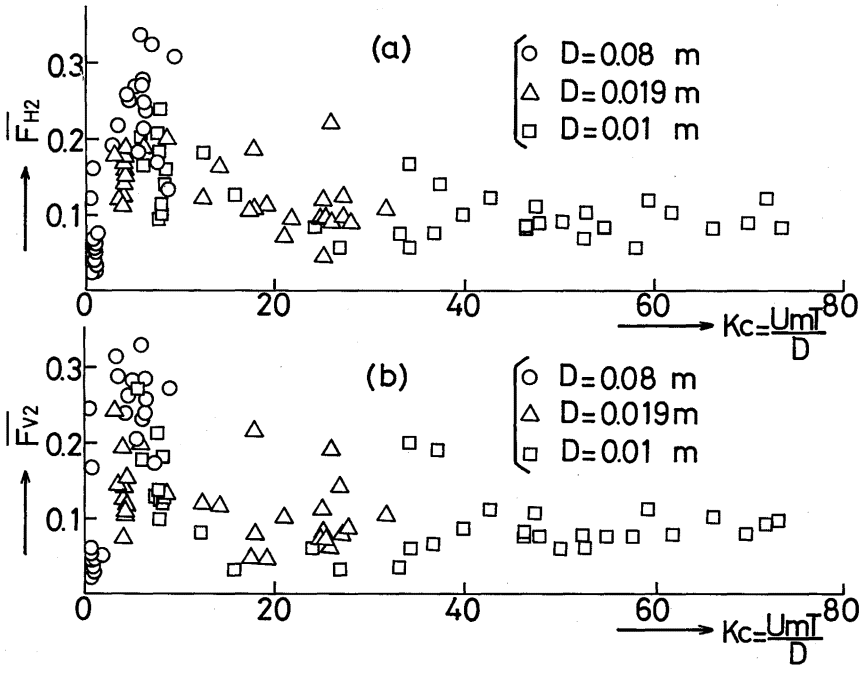

Fig. 13 Ratio of the amplitude of second order force to that of first order force, $\overline{F}_{H2}$, $\overline{F}_{V2}$

$$\left.\begin{aligned}\bar{F}_{H2}&=\frac{|\boldsymbol{F}_{H2}|}{|\boldsymbol{F}_{H1}|}\\ \bar{F}_{V2}&=\frac{|\boldsymbol{F}_{V2}|}{|\boldsymbol{F}_{V1}|}\end{aligned}\right\} \tag{19}$$

It is very interesting that these second order forces show the same tendency as the drag forces do, and it may be deduced that the second order forces are mainly due to vortices around the cylinder. The third order forces are smaller than 10 percents of total wave forces through all experiments.

4. Conclusions

The wave forces acting on horizontal submerged circular cylinders in deep waves are investigated. The following conclusions can be drawn from the present investigation.

1) In case of $K_c<30$, the drag coefficients in deep waves are rather different from those in oscillating fluid. In case of $K_c>30$, the drag coefficients in each experiment agree with that in steady flow.

2) The calculated inertia forces by linear theory show good agreement with experimental results at $K_c<1$. The calculated results are greater than experimental ones at large K_c. The inertia coefficients obtained by experiments at $K_c>20$ do not vary with K_c.

3) The calculated results of total wave force by linear theory show good agreement with the experimental ones at $K_c<1$. But in case of $1<K_c<10$, the calculated results are greater than experimental ones. In case of $K_c>10$, the calculated results are smaller than experimental ones.

4) The second order forces are large in the range where the drag forces are large. The third order forces are very small.

Acknowledgement

The author wishes to thank Mr. T. Nakajima, Mr. M. Sawada, Dr. F. Tasai, Dr. K. Kawatate and Dr. M. Ohkusu for valuable discussions. The skilled experimental assistance of Mr. A. Tasiro, Mr. T. Sinozaki and Mr. H. Nakamura is gratefully acknowledged. He would like to thank Mr. T. Nagahama and Miss. N. Sugino for assitance in preparing the manuscript.

Reference

1) Morison, J.R., et al.: The Force Exerted by Surface Waves on Piles, Petroleum Trans., Vol. 189 (1950).

2) Keulegan, G.H. and Carpenter, L.H.: Force on Cylinders and Plates in an Oscillating Fluid, Journal of Research of the National Bureau of Standards, Research

Paper No. 2857, Vol. 60, No. 5, May (1958).
3) Sarpkaya, T.: Force on Cylinder and Spheres in a sinusoidally Oscillating Fluid, Journal of Applied Mechanics, ASME, Vol. 42, No. 1, March (1975).
4) Sarpkaya, T.: Vortex Shedding and Resistance in Harmonic Flow about Smooth and Rough Circular Cylinders, Proceedings of an International Conference Boss '76 (1976).
5) Goda, Y.: Wave Force on a Vertical Cylinder; Experiments and a proposed Method of Wave Force Computation, Report of Port and Harbour Tech. Res. Inst., No. 8 (1964).
6) Tsuchiya, Y. and Yamaguchi, M.: Total Wave Force on a Vertical Circular Cylindrical Pile, Proceedings of the Japan Society of Civil Engineers, No. 227 (1974).
7) Bidde, D. D.: Laboratory Study of Lift Forces on Circular Piles, Journal of Waterways, Harbors and Coastal Engineering Division, ASCE, ww4 (1971).
8) Sawaragi, T., et al.: The Lifting Force on a Circular Cylinder, Proc. 22th Conf. Coast. Eng. in Japan (1975).
9) Nakaguchi, H.: Static Wind Load on Towers of Frame Work Structure, Journal of Japan Society for aeronautical Science, Vol. 12 (1964).
10) Tasai, F.: Dynamic Response of Floating Body in Waves, Symposium on the Ocean Engineering, S. N. A. of Japan (1974).
11) Takaki, M.: On the Ship Motions in Sallow Water (Part 1), Journal of the Society of Naval Architects of West Japan, Vol. 50 (1975).
12) Schlichting, H.: Boundary Layer Theory, Mc Graw-Hill Book Company, Inc., New York, N. Y., fourth edition (1960).
13) Schwabe, M.: Über Druckermittlung in der Instationnären ebenen Strömung, Ing. -Arch. 6, 34 (1935).
14) Honji, H. and Taneda, S.: Unsteady Flow past a Circular Cylinder, J. Phys. Soc. Japan, Vol. 27, No. 6 (1969).

(Received June 13, 1979)